PHYSICAL REVIEW D **94,** 034025 (2016)

Thermal relaxation, electrical conductivity, and charge diffusion in a hot QCD medium

Sukanya Mitra* and Vinod Chandra†

Indian Institute of Technology Gandhinagar, Gandhinagar-382355 Gujarat, India

(Received 28 June 2016; published 11 August 2016)

The response of electromagnetic (EM) fields that are produced in noncentral heavy-ion collisions to electromagnetically charged quark gluon plasma can be understood in terms of charge transport and charge diffusion in the hot QCD medium. This article presents a perspective on these processes by investigating the temperature behavior of the related transport coefficients, viz. electrical conductivity and the charge diffusion coefficients along with charge susceptibility. In the process of estimating them, thermal relaxation times for quarks and gluons have been determined first. These transport coefficients have been studied by solving the relativistic transport equation in the Chapman-Enskog method. For the analysis, $2 \to 2$, quark-quark, quark-gluon and gluon-gluon scattering processes are taken into account along with an effective description of hot QCD equations of state (EOSs) in terms of temperature dependent effective fugacities of quasiquarks (antiquarks) and quasigluons. Both improved perturbative hot QCD EOSs at high temperature and a lattice QCD EOS are included for the analysis. The hot QCD medium effects entering through the quasiparticle momentum distributions along with an effective coupling, are seen to have significant impact on the temperature behavior of these transport parameters along with the thermal relaxation times for the quasigluons and quasiquarks.

DOI: 10.1103/PhysRevD.94.034025

I. INTRODUCTION

Quantum chromodynamics (QCD)—the underlying theory of strong interaction in nature—predicts a deconfined state of the nuclear matter at high temperature (higher than QCD transition temperature T_c). Relativistic heavy-ion collision experiments at RHIC, BNL and LHC, CERN have reported the presence of near perfect liquid like hot nuclear matter [1,2] which turns out to be strongly coupled quark-gluon plasma (QGP). The QGP possesses a very tiny value of the shear viscosity to entropy density ratio, η/S (a few times the KSS bound [3]). The η/S has a lower bound near the transition temperature T_c as shown by several studies on QCD matter based on various approaches and the shear viscosity to entropy density ratio for the QGP is found to be lowest among all the known fluids [4,5]. In contrast, the bulk viscosity to entropy density ratio, ζ/S shows an upper bound with large values [6].

There has been growing interest in understanding the impact of strong electromagnetic (EM) fields that are produced during the initial stages of the noncentral heavy ion collisions [7], while investigating the hadronic observables at the later stages of the collisions. The impact of the EM field will be certainly dependent on the strength of the fields at the later stages as they are seen to decay quite rapidly [8]. The response of such EM fields (electrical) to the electromagnetically charged QGP can be understood in terms of the electrical conductivity, σ_{el} which characterizes the transport of the $U(1)$ conserved charge in the presence of the gradient of a charge chemical potential. There are several recent attempts to understand the σ_{el} in the context of EM field in RHIC [8–11]. The electrical conductivity in the context of charge fluctuations in heavy-ion collisions is investigated in [12]. Moreover, there are recent proposals to extract the electrical conductivity from the flow parameters in heavy ion collisions [13].

The other relevant, associated physical process is the charge diffusion, that is being quantified by the charge diffusion coefficient, D. The electrical conductivity, σ_{el} and the diffusion coefficient D are related by the famous Einstein relation through the charge susceptibility, χ.

The prime focus of this work is to estimate all these quantities for a hot QCD/QGP medium (their temperature dependence) which is characterized by an effective quasiparticle model. At this juncture, one needs to demarcate between the comoving frames while modeling expanding QGP medium, one with moving charge density and the other one with energy density. This requires the introduction of thermal conductivity which characterizes the flow associated with the transport of energy in response to the temperature gradient relative to locally comoving frames with the charge density. There are some recent attempts in the direction [14,15], however, our work in this manuscript does not involve any such investigation. As there are two equivalent approaches to estimate the transport coefficients of the hot QCD/QGP medium, viz., the linear response theory where one could relate them to the current-current spectral functions in thermal equilibrium through the Green-Kubo formulas [16], the other one is to solve a linearized transport equation in the presence of electric field along with an appropriate collision term (again linearized)

*sukanyam@iitgn.ac.in
†vchandra@iitgn.ac.in

and invoke pertinent equations of motion (for example Maxwell's equations in the case of electrical conductivity and electrical permittivities). The former approach best suited to lattice QCD estimations of the electrical conductivity and charge diffusion coefficient. There are several attempts from lattice QCD side to obtain the temperature dependence of the conductivity and charge diffusion coefficient [17–20,22–24] along with charge susceptibility [21]. The present work follows the latter approach based on the linearized transport equation.

There are a number of estimations of electrical conductivity (σ_{el}) by different approaches available in current literatures. In Refs. [25–27] the electrical conductivity has been estimated by solving the relativistic transport equation. In Refs. [28,29] the σ_{el} has been studied using off-shell parton-hadron string dynamics transport approach for an interacting system. In Ref. [30] σ_{el} as a function of temperature has been estimated using the maximum entropy method (MEM). Electrical conductivity along with diffusion coefficient and charge susceptibility has been estimated employing holographic technique in Ref. [31]. Recently the electrical conductivity has been studied including the momentum space anisotropy also [32]. In the hadronic sector also these quantities have been investigated lately. In Ref. [33] the electrical conductivity has been evaluated for a pion gas where in Ref. [34] the same has been studied for hot hadron gas.

While setting up an appropriate transport equation with a collision term for the determination of σ_{el} and D for the QGP medium, one must have a reliable modeling of the equilibrium state of the medium. To that end, quasiparticle descriptions of hot QCD medium play an important role. We employ such a model which is based on mapping the hot QCD medium effects encoded in the equation of state to the noninteracting/weakly interacting quasiparton degrees of freedom with temperature dependent effective fugacity parameter [35,36]. Further, the model can be understood in terms of renormalization of charges of quasipartons in the hot QCD medium. This enables us to define an effective coupling constant in hot QCD medium. The effective coupling thus obtained is employed in our analysis.

The manuscript is organized as follows. Section II offers mathematical formalism to determine thermal relaxation times for quasipartons (quasiquarks/antiquarks and quasigluons) followed by the analytical estimations of the transport coefficients, σ_{el}, D and χ. Section III deals with important predictions of the transport coefficients mentioned and related discussions. Finally, in Section IV, the conclusions and outlook of the work are presented.

II. FORMALISM

A. Quasiparticle description of hot QCD medium

Realization of hot QCD medium effects in terms of effective quasiparticle models has been there since the last few decades. In fact, there are various quasiparticle descriptions *viz.*, effective mass models [37,38], effective mass models with Polyakov loop [39], NJL and PNJL based effective models [40], and effective fugacity quasiparticle model (EQPM) description of hot QCD [35,36]. The present analysis considers the EQPM for the investigations on the properties of hot and dense medium in RHIC.

There are a number of estimations for different transport coefficients available in current literature which employ various quasiparticle models [41–43]. In Ref. [41], η and ζ have been evaluated for pure gluon plasma employing the effective mass quasiparticle model. On the other hand, in Refs. [42,43], η and ζ are obtained in gluonic as well as matter sector. References [44,45] presented the quasiparticle theory of η and ζ and their estimations for the hadronic sector. The thermal conductivity has also been studied, in addition to the viscosity parameters [45], within the effective mass model. In Ref. [46], the ratio of electrical conductivity to shear viscosity has been investigated within the framework of quasiparticle approach as well. However, these model calculations are not able to exactly reproduce the shear and bulk viscosities phenomenologically extracted from the hydrodynamic simulations of the QGP [47,48], consistently agreeing with different experimental observables measured like the multiplicity, transverse momentum spectra and the integrated flow harmonics of charged hadrons. Nevertheless, these quasiparticle approached could be useful in the equilibrium modeling of the hot QCD/QGP. The predictions based on these models are still useful in the sense of estimating some possible values these transport coefficients from some theoretical models that can considerably describe the interacting system created in heavy ion collisions.

1. The EQPM

The EQPM employed here, models the hot QCD in terms of effective quasipartons (quasigluons, quasiquarks/antiquarks). The model is based on the idea of mapping the hot QCD medium effects present in the equations of state (EOSs) either computed within improved perturbative QCD or lattice QCD simulations, into the effective equilibrium distribution functions for the quasipartons. The EQPM for the QCD EOS at $O(g^5)$ (EOS1) and $O(g^6\ln(1/g)+\delta)$ (EOS2) have been considered here. Additionally, the EQPM for the recent $(2+1)$-flavor lattice QCD EoS [49] at physical quark masses (LEOS), has been employed for our analysis. There are more recent lattice results with the improved actions and refined lattices [50], for which we need to relook at the model with specific set of lattice data specially to define the effective gluonic degrees of freedom. Therefore, we will stick to the set of lattice data utilized in the model described in Ref. [36].

In either of the cases of above mentioned EOSs, the form of the quasiparton equilibrium distribution functions, $f_{eq} \equiv \{f_g, f_q\}$ (describing the strong interaction effects in terms of effective fugacities $z_{g,q}$) can be written as.

$$f_{g/q} = \frac{z_{g/q}\exp[-\beta E_p]}{(1 \mp z_{g/q}\exp[-\beta E_p])} \tag{1}$$

where $E_p = |\vec{p}|$ for the gluons and $\sqrt{|\vec{p}|^2 + m_q^2}$ for the quark degrees of freedom (m_q denotes the mass of the quarks), and $\beta = T^{-1}$ denotes inverse of the temperature. We use the notation $\nu_g = 2(N_c^2 - 1)$ for gluonic degrees of freedom, $\nu_q = 4N_cN_f$ for $SU(N_c)$ with N_f number of flavors. As we are working at zero baryon chemical potential, therefore quark and antiquark distribution functions are the same. Since the model is valid in the deconfined phase of QCD (beyond T_c), therefore, the mass of the light quarks can be neglected as compared to the temperature. As QCD is a $SU(3)$ gauge theory so $N_c = 3$ for our analysis. Noteworthily, the EOS1 which is fully perturbative, is proposed by Arnold and Zhai [51] and Zhai and Kastening [52]. On the other hand, EOS2 which is at $O(g^6\ln(1/g) + \delta)$ is determined by Kajantie *et al.* [53] while incorporating contributions from nonperturbative scales such as gT and g^2T. Notably, these effective fugacities ($z_{g/q}$) are not merely temperature dependent parameters that encode the hot QCD medium effects; they lead to nontrivial dispersion relation both in the gluonic and quark sectors as,

$$\omega_{g/q} = E_p + T^2\partial_T ln(z_{g/q}), \tag{2}$$

where $\omega_{g,q}$ denote the quasigluon and quasiquark dispersions (single particle energy), respectively. The second term in the right-hand side of Eq. (2), encodes the effects from collective excitations of the quasipartons.

The effective fugacities, z_g, z_q are not related with any conserved number current in the hot QCD medium. They have been merely introduced to encode the hot QCD medium effects in the EQPM. The physical interpretation of z_g and z_q emerges from the above mentioned nontrivial dispersion relations. The modified part of the energy dispersions in Eq. ((2) leads to the trace anomaly (interaction measure) in hot QCD and takes care of the thermodynamic consistency condition. It is straightforward to compute gluon and quark number densities and all the thermodynamic quantities such as energy density, entropy, enthalpy etc. by realizing hot QCD medium in terms of an effective grand canonical system [35,36]. Furthermore, these effective fugacities lead to a very simple interpretation of hot QCD medium effects in terms of an effective virial expansion. Note that $z_{g,q}$ scales with T/T_c, where T_c is the QCD transition temperature.

The number densities, n_g (for gluons), n_q (for quarks, antiquarks) are obtained from Eq. (1) as,

$$n_g = \frac{\nu_g}{(2\pi)^3}\int d^3\vec{p} f_g(\vec{p}) = \frac{\nu_g T^3}{\pi^2}\text{PolyLog}[3, z_g], \tag{3}$$

$$n_q = \frac{\nu_q}{(2\pi)^3}\int d^3\vec{p} f_q(\vec{p}) = \frac{-\nu_q T^3}{\pi^2}\text{PolyLog}[3, -z_q]. \tag{4}$$

The number densities approach to their Stefan-Boltzmann (SB) limit only asymptotically (*i.e* $z_{g,q} \to 1$). On the other hand, the pressure, $P \equiv P_g + P_q$, Energy density, $\epsilon = \epsilon_g + \epsilon_q$ can be obtained from the relation:

$$P_{g,q} = \mp\nu_{g,q}\int\frac{d^3p}{(2\pi)^3}\ln(1 \mp z_{g,q}\exp(-\beta E_p)) = \pm\frac{\nu_{g,q}T^4}{\pi^2}\text{PolyLog}[4, \pm z_{g,q}], \tag{5}$$

$$\epsilon_{g,q} = \nu_{g,q}\int\frac{d^3p}{(2\pi)^3}\omega_{g,q}f_{g,q} = \pm\frac{3\nu_{g,q}T^4}{\pi^2}\text{PolyLog}[4, \pm z_{g,q}] \pm\frac{T^4\nu_{g,q}}{\pi^2}T\partial_T\ln(z_{g,q})\text{PolyLog}[3, \pm z_{g,q}]. \tag{6}$$

The first term in the right-hand side of Eq. (6) is nothing but the $3P_{g,q}$, while second term leads to nonvanishing interaction measure in hot QCD. The entropy density and enthalpy can be read off from the expressions of ϵ and P using well known thermodynamic relations. The energy density and enthalpy density per particle can easily obtained employing results from Eqs. (3)–(6).

2. Charge renormalization and effective coupling

In contrast to the effective mass models where the effective mass is motivated from the mass renormalization in the hot QCD medium, the EQPM is based on the charge renormalization in high temperature QCD.

To investigate how the quasi partonic charges modify in the presence of hot QCD medium, we consider the expression for the Debye mass derived in semi-classical transport theory [54–56] as,

$$m_D^2 = 4\pi\alpha_s(T)\left(-2N_c\int\frac{d^3p}{(2\pi)^3}\partial_p f_g(\vec{p}) + 2N_f\int\frac{d^3p}{(2\pi)^3}\partial_p f_q(\vec{p})\right), \tag{7}$$

where, $\alpha_s(T)$ is the QCD running coupling constant at finite temperature [57].

After performing the momentum integral after substituting the quasiparton distribution function from Eq. (1) to Eq. (7), we obtain,

$$m_D^2 = 4\pi\alpha_s(T)T^2\left(\frac{2N_c}{\pi^2}\text{PolyLog}[2,z_g] - \frac{2N_f}{\pi^2}\text{PolyLog}[2,-z_q]\right). \quad (8)$$

The Debye mass here reduces to the leading order HTL expression in the limit $z_{g,q}=1$ (ideal EoS: noninteracting of ultra relativistic quarks and gluons),

$$m_D^2(\text{HTL}) = \alpha_s(T)T^2\left(\frac{N_c}{3}+\frac{N_f}{6}\right). \quad (9)$$

Equation (8) can be rewritten as,

$$m_D^2 = m_D^2(\text{HTL}) \times \frac{\frac{2N_c}{\pi^2}\text{PolyLog}[2,z_g] - \frac{2N_f}{\pi^2}\text{PolyLog}[2,-z_q]}{\frac{N_c}{3}+\frac{N_f}{6}}. \quad (10)$$

We can now define the effective coupling, $\alpha_{\text{eff}} \equiv \alpha_s(T)g(z_g,z_q)$, so that the $m_D^2 = 4\pi\alpha_{\text{eff}}(T)T^2(N_c/3+N_f/6)$. The function $g(z_g,z_q)$ reads,

$$g(z_g,z_q) = \frac{\frac{2N_c}{\pi^2}\text{PolyLog}[2,z_g] - \frac{2N_f}{\pi^2}\text{PolyLog}[2,-z_q]}{\frac{N_c}{3}+\frac{N_f}{6}}. \quad (11)$$

Notably, the EQPM employed here has been remarkably useful in understanding the bulk and the transport properties of the QGP in heavy-ion collisions [42,43,58–60].

The behavior of the ratio $\alpha_{\text{eff}}/\alpha_s \equiv g(z_g,z_q)$ as a function of temperature (T/T_c) for various EOSs is depicted in Fig. 1. The flavor dependence is also shown in Fig. 1. Clearly the ratio will approach its value with ideal EOS ($z_{g,q}\to 1$) which is unity, only asymptotically. The EOS dependence can clearly be visualized from the temperature dependence of the relative coupling in Fig. 1. For example the LEOS result is closest to the running α_s among all the cases. Similiary, other EOS dependent predictions can also be explicated.

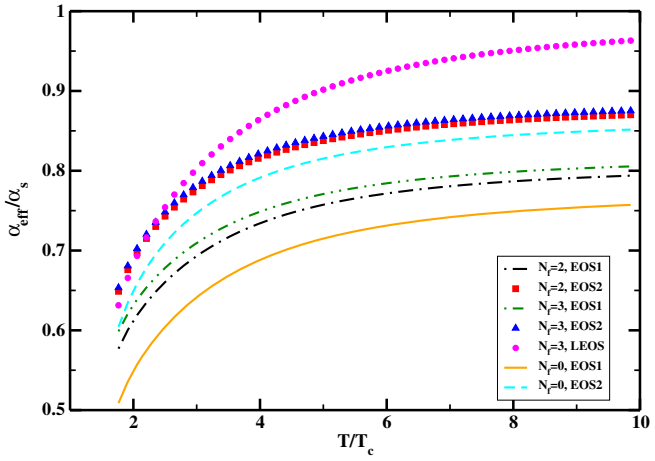

FIG. 1. Effective coupling constant using various EOS as a function of T/T_c.

There are only two free functions (z_g, and z_q) in the EQPM employed here which depend on the chosen EOS. In the case of EOS1 and EOS2 employed in the present case, these functions are obtained in [35] and are continuous functions of T/T_c. On the other hand, for LEOS they are defined in terms of eight parameters obtained in Ref. [36] (See Table I of Ref. [36]). Apart from that effective coupling mentioned above depends on them and the QCD running coupling constant $g(T)$, that explicitly depends upon how we fix the QCD renormalization scale at finite temperature and up to what order we define $g(T)$. Henceforth, these are the three quantities that need to be supplied throughout the analysis here.

B. Thermal relaxation times

In order to estimate the relaxation times of particles due to their mutual interactions we start with the Boltzmann transport equation for an out of equilibrium system that describes the binary elastic process $p_k + p_l \to p_k' + p_l'$,

$$\frac{df_k(x,p_k)}{dt} = -C[f_k]. \quad (12)$$

Here f_k is the single particle distribution function for the k^{th} species in a multicomponent system, that depends upon the particle 4-momentum p_k and 4-space-time coordinates x. $C[f_k]$ denotes the collision term that quantifies the rate of change of f_k given in the following manner [61],

$$\begin{aligned} C[f_k] = \frac{1}{2}\nu_l\sum_{l=1}^{N}\frac{1}{2\omega_k}\int d\Gamma_{p_l}d\Gamma_{p_k'}d\Gamma_{p_l'}(2\pi)^4 \\ \times \delta^4(p_k+p_l-p_k'-p_l')\langle|M_{k+l\to k+l}|^2\rangle \\ \times [f_k(p_k)f_l(p_l)\{1\pm f_k(p_k')\}\{1\pm f_l(p_l')\} \\ - f_k(p_k')f_l(p_l')\{1\pm f_k(p_k)\}\{1\pm f_l(p_l)\}] \\ k = 1,2,\ldots,N. \end{aligned} \quad (13)$$

The phase space factor is expressed by the notation $d\Gamma_{p_i} = \frac{d^3\vec{p}_i}{(2\pi)^3 2\omega_i}$, as ω_k is the energy of the scattered particle which is of kth species. The overall $\frac{1}{2}$ factor is appearing due to the symmetry in order to compensate for the double counting of final states that occurs by interchanging p_k' and p_l'. ν_l is the degeneracy of 2nd particle that belongs to lth species. It is considered next that the out of equilibrium distribution function of the 1st particle, which is being scattered is given by,

$$f_k = f_k^0 + \delta f_k = f_k^0 + f_k^0(1 \pm f_k^0)\phi_k, \tag{14}$$

where the nonequilibrium part δf_k of the distribution function is quantified by the deviation function ϕ_k. The collision term can now be expressed as the distribution deviation over the relaxation time τ_k, which is needed by the out of equilibrium distribution function to restore its equilibrium value,

$$C[f_k] = \frac{\delta f_k}{\tau_k} = \frac{f_k^0(1 \pm f_k^0)\phi_k}{\tau_k}. \tag{15}$$

Putting (14) into the right-hand side of (13) by keeping the distribution functions of the particles other than the scattered one vanishingly close to equilibrium and comparing with (15), the relaxation time finally becomes as the inverse of the reaction rate Γ_k of the respective processes [62],

$$\begin{aligned}\tau_k^{-1} &\equiv \Gamma_k \\ &= \frac{\nu_l}{2}\frac{1}{2\omega_k}\int d\Gamma_{p_l} d\Gamma_{p_k'} d\Gamma_{p_l'} (2\pi)^4 \delta^4(p_k + p_l - p_k' - p_l') \\ &\quad \times \langle |M_{k+l\to k+l}|^2 \rangle \frac{f_l'^0(1 \pm f_k'^0)(1 \pm f_l^0)}{(1 \pm f_k^0)}.\end{aligned} \tag{16}$$

Clearly the distribution function of final state particles are given by primed notation.

Simplifying τ_k utilizing the δ-function we finally obtain τ_k in the center of momentum frame of particle interaction as,

$$\tau_k^{-1} = \Gamma_k = \nu_l \int \frac{d^3\vec{p}_l}{(2\pi)^3} d(\cos\theta) \frac{d\sigma}{d(\cos\theta)} \frac{f_l'^0(1 \pm f_k'^0)(1 \pm f_l^0)}{(1 \pm f_k^0)}, \tag{17}$$

where θ is the scattering angle in the center of momentum frame and σ is the interaction cross section for the respective scattering processes. Now in terms of the Mandelstam variables s, t, and u the expression for τ_k can be reduced simply as,

$$\tau_k^{-1} = \Gamma_k = \nu_l \int \frac{d^3\vec{p}_l}{(2\pi)^3} dt \frac{d\sigma}{dt} \frac{f_l'^0(1 \pm f_k'^0)(1 \pm f_l^0)}{(1 \pm f_k^0)}. \tag{18}$$

The differential cross section relates the scattering amplitudes as $\frac{d\sigma}{dt} = \frac{\langle |M|^2 \rangle}{16\pi s^2}$. The quark-gluon scattering amplitudes for $2 \to 2$ processes are taken from [63], that are averaged over the spin and color degrees of freedom of the initial states and summed over the final states.

Now in order to take into account the small-angle scattering scenario that results into divergent contributions from t-channel diagrams of QCD interactions, a transport weigh factor $(1 - \cos\theta) = \frac{2tu}{s^2}$ have been introduced in the interaction rate [64,65]. Furthermore considering the momentum transfer $q = |\vec{p}_k - \vec{p}_k'| = |\vec{p}_l - \vec{p}_l'|$ is not too large we can make the following assumptions, $f_k^0 \cong f_k'^0$ and $f_l^0 \cong f_l'^0$ [64] to finally obtain,

$$\tau_k^{-1} = \Gamma_k = \nu_l \int \frac{d^3\vec{p}_l}{(2\pi)^3} f_l^0(1 \pm f_l^0) \int dt \frac{d\sigma}{dt}\frac{2tu}{s^2}. \tag{19}$$

In the integration involving t-channel diagrams from where the infrared logarithmic singularity appears, the limit of integration is restricted from $-s$ to $-k^2$ in order to avoid those divergent results using the cutoff $k^2 = g^2T^2$ as infrared regulator. Here $g^2 = 4\pi\alpha_s$ with α_s being the coupling constant of strong interaction as already mentioned in Sec. A.

Now in the QGP medium the quark and gluon interaction rates result from the following interactions respectively,

$$\Gamma_g = \Gamma_{gg} + \Gamma_{gq}, \qquad \Gamma_q = \Gamma_{qg} + \Gamma_{qq}, \tag{20}$$

where Γ_{gg}, Γ_{gq}, Γ_{qg} and Γ_{qq} are the interaction rates between gluon-gluon, gluon-quark, quark-gluon and quark-quark, respectively.

Finally after pursuing the angular integration in (19) we are left with the thermal relaxation times of the quark and gluon components in a QGP system in the following way,

$$\begin{aligned}\tau_g^{-1} &= \left\{\nu_g \int \frac{d^3\vec{p}_l}{(2\pi)^3} f_g^0(1 + f_g^0)\right\} \\ &\quad \times \left[\frac{9g^4}{16\pi\langle s\rangle_{gg}}\left\{ln\frac{\langle s\rangle_{gg}}{k^2} - 1.267\right\}\right] \\ &\quad + \left\{\nu_q \int \frac{d^3\vec{p}_l}{(2\pi)^3} f_q^0(1 - f_q^0)\right\} \\ &\quad \times \left[\frac{g^4}{4\pi\langle s\rangle_{gq}}\left\{ln\frac{\langle s\rangle_{gq}}{k^2} - 1.287\right\}\right],\end{aligned} \tag{21}$$

$$\begin{aligned}\tau_q^{-1} &= \left\{\nu_g \int \frac{d^3\vec{p}_l}{(2\pi)^3} f_g^0(1 + f_g^0)\right\} \\ &\quad \times \left[\frac{g^4}{4\pi\langle s\rangle_{qg}}\left\{ln\frac{\langle s\rangle_{qg}}{k^2} - 1.287\right\}\right] \\ &\quad + \left\{\nu_q \int \frac{d^3\vec{p}_l}{(2\pi)^3} f_q^0(1 - f_q^0)\right\} \\ &\quad \times \left[\frac{g^4}{9\pi\langle s\rangle_{qq}}\left\{ln\frac{\langle s\rangle_{qq}}{k^2} - 1.417\right\}\right],\end{aligned} \tag{22}$$

where $\langle s\rangle_{kl} = 2\langle p_k\rangle\langle p_l\rangle$ is the thermal average value of s with $\langle p_k\rangle = \frac{\int \frac{d^3\vec{p}_k}{(2\pi)^3}|\vec{p}_k| f_k^0}{\int \frac{d^3\vec{p}_k}{(2\pi)^3} f_k^0}$. Clearly in order to account for a hot QCD medium the quasiparticle effects must be invoked in the expressions of these thermal relaxation times obtained

far. As discussed in Sec. A, the distribution functions of quarks and gluons and the coupling g will carry the quasiparticle descriptions accordingly. Since the cutoff parameter k also depends upon g and the thermal average of s includes $f^0_{g/q}$, they will reflect the hot QCD equation of state effect as well. Following the definition of equilibrium distribution function of quarks and gluons from Eq. (1), within the quasiparticle framework, the thermal averages of gluon and quark momenta respectively are obtained as,

$$\langle p_g \rangle = 3T \frac{\text{PolyLog}[4, z_g]}{\text{PolyLog}[3, z_g]}, \tag{23}$$

$$\langle p_q \rangle = 3T \frac{\text{PolyLog}[4, -z_q]}{\text{PolyLog}[3, -z_q]}. \tag{24}$$

C. Electrical conductivity

In this work, we have adopted the kinetic theory approach for evaluating the analytical expression of electrical conductivity, based on solving the relativistic transport equation for a charged QGP system.

Before proceeding for the solution of a transport equation, we introduce here some of the thermodynamic quantities needed for developing the required framework. We start with particle 4-flow for the kth species of particle in a multicomponent system [66],

$$N^\mu_k(x) = \int \frac{d^3\vec{p}_k}{(2\pi)^3 p^0_k} p^\mu_k f_k(x, p_k). \tag{25}$$

Next the total particle 4-flow and the energy momentum tensor of the system are defined, respectively, as the following,

$$N^\mu(x) = \sum_{k=1}^{N} N^\mu_k(x) = \sum_{k=1}^{N} \int \frac{d^3\vec{p}_k}{(2\pi)^3 p^0_k} p^\mu_k f_k(x, p_k), \tag{26}$$

$$T^{\mu\nu}(x) = \sum_{k=1}^{N} \int \frac{d^3\vec{p}_k}{(2\pi)^3 p^0_k} p^\mu_k p^\nu_k f_k(x, p). \tag{27}$$

With the help of the above quantities we define the diffusion flow of the kth component as [66],

$$I^\mu_k = N^\mu_k - x_k N^\mu, \tag{28}$$

where $x_k = \frac{n_k}{n}$ is the particle fraction corresponding to kth species, n_k and n are the particle number density for kth species and total particle number density of the multicomponent system respectively, which are related by $n = \sum_{k=1}^{N} n_k$. We can readily notice $\sum_{k=1}^{N} I_k = 0$, i.e., sum of the diffusion flows vanishes.

The total electric current density of such a system is given by [67],

$$J^\mu(x) = \sum_{k=1}^{N} q_k I^\mu_k = \sum_{k=1}^{N-1} (q_k - q_N) I^\mu_k, \tag{29}$$

where q_k is the electric charge associated with the kth species.

A realistic description of nonequilibrium phenomena in relativistic systems must take reactive processes into account which incorporates all kinds of inelastic collisions beside elastic ones. In such a case the system must include a number of conserved quantum numbers and the diffusion flow in such situations will become,

$$I^\mu_a = \sum_{k=1}^{N} q_{ak} I_k, \qquad [a = 1, 2, \ldots N'] \tag{30}$$

$$= \sum_{k=1}^{N} q_{ak} \{N^\mu_k - x_k N^\mu\}. \tag{31}$$

Here a stands for the index of conserved quantum number and q_{ak} is the ath conserved quantum number associated with kth component. Following the prescription we are able to define the particle number density of the independent components as, $n_a = \sum_{k=1}^{N} q_{ak} n_k$.

After defining these basic thermodynamic quantities let us present the relativistic transport equation (12) in covariant form with the force term present in it [25],

$$p^\mu_k \partial_\mu f_k + q_k F^{\alpha\beta} p_\beta \frac{\partial f_k}{\partial p^\alpha_k} = -C[f_k]. \tag{32}$$

Here $F^{\mu\nu} = \{-u^\mu E^\nu + u^\nu E^\mu\}$ is the electromagnetic field tensor with electric field E^μ, in the absence of any magnetic field in the medium. We identify u^μ as hydrodynamic 4-velocity. Throughout this paper we will use the metric system $g^{\mu\nu} = \{1, -1, -1, -1\}$.

Now using the Chapman-Enskog (CE) method the transport equation is linearized around a local equilibrium distribution function $f^0_k(x, p_k)$ and finally the CE hierarchy reduces the left-hand side of the transport equation in terms of f^0_k. The collision term is simplified using (15) giving rise to,

$$p^\mu_k \partial_\mu f^0_k + \frac{1}{T} f^0_k (1 \pm f^0_k) q_k E_\mu p^\mu_k = -\frac{\omega_k}{\tau_k} f^0_k (1 \pm f^0_k) \phi_k. \tag{33}$$

To proceed further the distribution functions of constituent particles is needed to be provided in covariant notations. In a comoving frame and involving the quasiparticle description discussed in Sec. A, it can be given in the following way,

$$f_k^0(x,p_k)=\frac{z_k\exp[-\frac{p_k^\mu u_\mu}{T}+\frac{\mu_k}{T}]}{1\mp z_k\exp[-\frac{p_k^\mu u_\mu}{T}+\frac{\mu_k}{T}]}, \tag{34}$$

where we have introduced ω_k as the energy per particle of the kth species and μ_k is the chemical potential for the same. Within the quasiparticle framework, for quarks and gluons ω_k is defined by Eq. (2).

In order to retrieve the transport equation in terms of the thermodynamic forces, the first term on the left-hand side of Eq. (33) is needed to be reduced by decomposing the derivative over the distribution function into a timelike and a spacelike part as $\partial^\mu = u^\mu D + \nabla^\mu$, with the covariant time derivative $D = u^\mu\partial_\mu$ and the spatial gradient $\nabla_\mu = \Delta_{\mu\nu}\partial^\nu$, expressed in terms of hydrodynamic 4-velocity u^μ and projection operator $\Delta_{\mu\nu} = g_{\mu\nu} - u_\mu u_\nu$. Whence the spatial gradients over velocity, temperature, and chemical potentials directly link with the viscous flow, heat flow and the diffusion flow of the fluid, respectively, the time derivatives are needed to be eliminated using a number of thermodynamic identities so that they contribute in the expressions of the thermodynamic forces as well. The time derivative over particle number density and the time derivative over energy per particle however follow the equation of continuity and equation of energy as in the case of a system without the influence of electric field,

$$Dn_k = -n_k\partial\cdot u, \tag{35}$$

$$\sum_{k=1}^{N} x_k D\omega_k = -\frac{\sum_{k=1}^{N} P_k}{\sum_{k=1}^{N} n_k}\partial\cdot u, \tag{36}$$

where P_k is the partial pressure attributed to kth species. But the equation of motion in the presence of the electric field will be different from the one without electric field. In a multicomponent system in the presence of an electric field the equation of motion takes the following form,

$$Du^\mu = \frac{\nabla^\mu P}{\sum_{k=1}^{N} n_k h_k} + \frac{\sum_{k=1}^{N} q_k n_k}{\sum_{k=1}^{N} h_k n_k}E^\mu. \tag{37}$$

Clearly even the pressure gradient is zero, the Lorentz force acting on the particle produces nonzero acceleration. By utilizing these identities and retaining the thermodynamic forces involving thermal and diffusion terms only, (shear and bulk viscous part not considered in this work), the transport equation becomes,

$$\frac{1}{T}\left[p_k^\nu\{(p_k.u)-h_k\}X_{qk}+p_k^\nu\sum_{a=1}^{N'-1}(q_{ak}-x_a)X_{a\nu}\right]=-\frac{\omega_k}{\tau_k}\phi_k, \tag{38}$$

where $X_{q\mu}$ and $X_{a\mu}$ are the thermal and diffusion forces respectively given by,

$$X_{q\mu}=\left[\frac{\nabla_\mu T}{T}-\frac{\nabla_\mu P}{nh}\right]+\left[-\frac{1}{h}\sum_{k=1}^{N}x_k q_k E_\mu\right], \tag{39}$$

$$X_{k\mu}=\left[(\nabla_\mu\mu_a)_{P,T}-\frac{h_k}{nh}\nabla_\mu P\right]+\left[q_k-q_N-\frac{h_k-h_N}{h}\sum_{l=1}^{N}x_l q_l\right]E_\mu. \tag{40}$$

The detail of the computation in offered in Appendix A.

We identify h_k and h as the enthalpy per particle for species k and for total system, respectively, and $(\nabla_\mu\mu_a)_{P,T}=\sum_{b=1}^{N'-1}\{\frac{\partial\mu_a}{\partial x_b}\}_{P,T,\{x_a\}}\nabla_\mu x_b$. Here x_a and μ_a are the particle fraction and chemical potential associated with ath quantum number respectively. Clearly in the expressions of thermal and diffusion driving forces, terms proportional to electric field give rise to electrical conductivity. Now in order to be a solution of this equation the deviation function ϕ_k must be a linear combination of the thermodynamic forces,

$$\phi_k = B_{k\mu}X_q^\mu + \frac{1}{T}\sum_{a=1}^{N'-1}B_{ak}^\mu X_{a\mu}, \tag{41}$$

with, $B_k^\mu = B_k\langle\Pi_k^\mu\rangle$ and $B_{ak}^\mu = B_{ak}\langle\Pi_k^\mu\rangle$ where $\langle\Pi_k^\mu\rangle = (\Pi_k)_\nu\Delta^{\mu\nu}$ and $\Pi_k = p_k/T$.

Putting (41) into the right-hand side of (38) and comparing both sides of (38) (noting thermodynamic forces are independent) we finally obtain,

$$B_k^\mu = \langle\Pi_k^\mu\rangle\frac{\omega_k-h_k}{\{-\frac{\omega_k}{\tau_k}\}}, \qquad B_{ak}^\mu = \langle\Pi_k^\mu\rangle\frac{q_{ak}-x_a}{\{-\frac{\omega_k}{\tau_k T}\}}, \tag{42}$$

from which the complete structure of ϕ_k can be obtained. Now going back to Eq. (31) we notice for equilibrium distribution function f_k^0 the I_a^μ clearly vanishes, while with $f_k = f_k^0(1\pm f_k^0)\phi_k$ it gives a finite diffusion flow as follows,

$$I_a^\mu = \sum_{k=1}^{N}(q_{ak}-x_a)\int\frac{d^3\vec{p}_k}{(2\pi)^3 p_k^0}p_k^\mu f_k^0(1\pm f_k^0)\phi_k. \tag{43}$$

Putting the value of ϕ_k from (41) with the help of Eqs. (42) into (43) we get the linear law of diffusion flow,

$$I_a^\mu = l_{aq}X_q^\mu + \sum_{b=1}^{N'-1}l_{ab}X_b^\mu, \qquad a=1,\ldots,(N'-1), \tag{44}$$

where the coefficients are now expressed in terms of the relaxation time τ,

$$l_{aq} = \sum_{k=1}^{N}(q_{ak} - x_a)\frac{1}{T}\int \frac{d^3\vec{p}_k}{(2\pi)^3} f_k^0(1 \pm f_k^0)\tau_k \times (\omega_k - h_k), \tag{45}$$

$$l_{ab} = \sum_{k=1}^{N}(q_{ak} - x_a)(q_{bk} - x_b)\frac{1}{T}\int \frac{d^3\vec{p}_k}{(2\pi)^3} f_k^0(1 \pm f_k^0)\tau_k. \tag{46}$$

Now substituting the expression of diffusion flow into Eq. (29), and pertaining the terms proportional to electric field only we finally reach the expression for the electric current density,

$$J^\mu = \sum_{k=1}^{N-1}(q_k - q_N)\left[\sum_{l=1}^{N-1} l_{kl}\left\{q_l - q_N - \frac{h_l - h_N}{h}\sum_{n=1}^{N} x_n q_n\right\} - \frac{l_{kq}}{h}\sum_{n=1}^{N} x_n q_n\right]E^\mu. \tag{47}$$

We also know the current density relates with the electric field by the linear relation via the electrical conductivity as,

$$J^\mu = \sigma_{el} E^\mu. \tag{48}$$

By comparing (47) and (48) we finally obtain the detailed expression of electrical conductivity in the following manner,

$$\sigma_{el} = \sum_{k=1}^{N-1}(q_k - q_N)\left[\sum_{l=1}^{N-1} l_{kl}\left\{q_l - q_N - \frac{h_l - h_N}{h}\sum_{n=1}^{N} x_n q_n\right\} - \frac{l_{kq}}{h}\sum_{n=1}^{N} x_n q_n\right]. \tag{49}$$

Now for a quark-gluon system the expression of the electric conductivity boils down to,

$$\sigma_{el} = q_q^2 \frac{l_{11}h_g - l_{1q}x_q}{h}. \tag{50}$$

The subscript q and g stands for quarks and gluons respectively. So finally we are left with the coefficients as,

$$l_{1q} = \frac{1}{T}\left[-x_q\tau_g\int \frac{d^3p_g}{(2\pi)^3} f_g^0(1 + f_g^0)(\omega_g - h_g) + x_g\tau_q\int \frac{d^3p_q}{(2\pi)^3} f_q^0(1 - f_q^0)(\omega_q - h_q)\right], \tag{51}$$

$$l_{11} = \frac{1}{T}\left[x_q^2\tau_g\int \frac{d^3p_g}{(2\pi)^3} f_g^0(1 + f_g^0) + x_g^2\tau_q\int \frac{d^3p_q}{(2\pi)^3} f_q^0(1 - f_q^0)\right]. \tag{52}$$

The $q_q^2 = \sum_k \nu_k q_{qk}^2$ is simply the square of the fractional quark charges taking sum over quark degeneracies. For up, down, and strange quarks the fractions quark charge is taken to be $2/3$, $-1/3$, and $-1/3$, respectively.

D. Charge diffusion

We recall Eq. (44), where the diffusion flow is linearly expressed in terms of thermal and diffusion driving forces respectively. The diffusion driving force does not include the terms containing $a = N'$ because diffusion flow vanishes for those values of a. Since presently we are dealing with a quark-gluon plasma which incorporates binary elastic collisions that conserve particle numbers, in such case the distinction between the independent particle fractions $x_a, a = 1, \ldots, N'$ and the particle fraction of separate components $x_k, k = 1, \ldots, N$ vanishes. So in the present situation the diffusion flow rather follows the relation $\sum_{k=1}^{N} I_k = 0$, as mentioned earlier. In such scenario the original diffusion driving forces (not containing the electric field) conjugate to (N-1) independent diffusion flows is given by [66],

$$X_k^\mu = [(\nabla^\mu\mu_k)_{P,T} - (\nabla^\mu\mu_N)_{P,T}] - \frac{h_k - h_N}{hn}\nabla^\mu P, \quad k = 1, 2, \ldots (N-1). \tag{53}$$

It is straightforward to prove that $(\nabla^\mu\mu_k)_{P,T} = \frac{T}{x_k}\nabla^\mu x_k$. Thus, in the absence of any electric field in X_k^μ, the flow becomes purely diffusive that encodes the spacial variation of the fractional particle density corresponding to different species. Finally, for a two component quark-gluon system at mechanical equilibrium, i.e., at vanishing pressure gradient we obtain the diffusion flow in the following way,

$$I_1^\mu = nx_q x_g D_T \nabla^\mu T + nD\nabla^\mu x_q. \tag{54}$$

So we are able to identify the diffusion coefficient as

$$D = \frac{Tl_{11}}{nx_q x_g}, \tag{55}$$

and the thermal diffusion coefficient as,

$$D_T = \frac{l_{1q}}{nx_q x_g T}. \tag{56}$$

Taking the value of l_{11} from (52) and incorporating the sum over all flavors and helicities of the quarks, interacting among themselves and gluons, we are finally able to estimate the charge diffusion coefficient of the system.

E. Charge susceptibility

In previous sections, we obtained both the expressions of electrical conductivity and flavor diffusion. In the absence

of any electric field, the out of equilibrium particle distribution function relaxes pure diffusively, whereas, in the presence of an electric field the restoration of equilibrium is affected by the electric conductivity. These two quantities are linearly related by Einstein's relation,

$$\sigma_{el} = \chi D, \tag{57}$$

where the proportionality constant is termed as charge susceptibility. Clearly this term is independent of the relaxation time τ and particle interactions. It depends upon the fractional quark charges and thermodynamic parameters describing the system. In transport theory this quantity is also of significant interest and hence studied in the present work.

III. RESULTS AND DISCUSSIONS

In this section, we initiate our discussions with the temperature dependence of the thermal relaxation times of quarks and gluons considering 3-flavors of quarks (up, down, and strange). Following from Eqs. (21) and (22), τ_g and τ_q have been plotted as a function of T/T_c for different α_s in Fig. 2 and Fig. 3, respectively. Both τ_g and τ_q exhibit the expected decreasing trend with increasing temperature. This observation reveals that at higher temperature, the increased interaction rates make the quarks and gluons to restore their equilibrium faster. The order of magnitude of τ_g and τ_q and the fact that τ_q is larger than τ_g agree with the work in [68]. The thermal relaxation times for both the cases have been estimated for different values of the QCD couplings.

First, we consider the situation where ideal EOS has been used in the definition of the distribution functions to be implemented in the expressions of τ's. In this case both a fixed value of coupling, $\alpha_s = 0.3$ (indicated by the black circles) and the temperature dependent running coupling

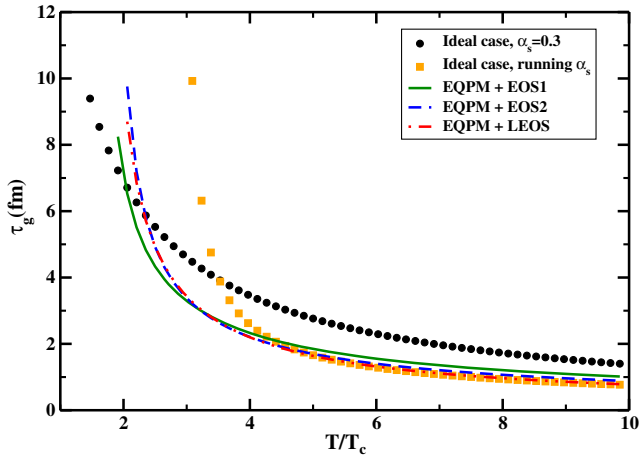

FIG. 2. Temperature dependence of thermal relaxation times for gluons for 3- flavor case.

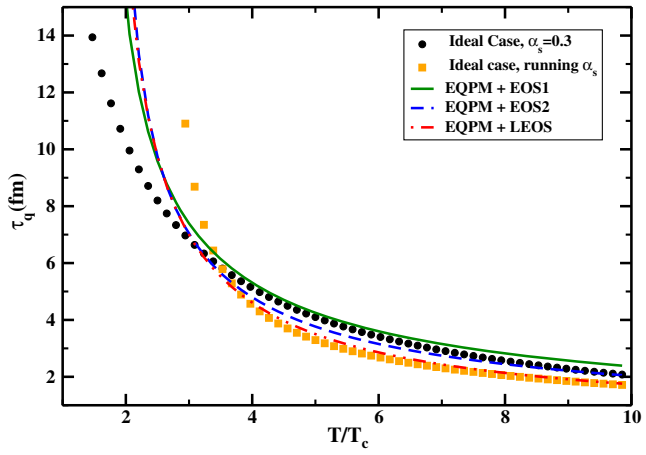

FIG. 3. Temperature dependence of thermal relaxation times for quarks for 3-flavor case.

$\alpha_s(T)$ (indicated by the orange squares) have been used. The large values of τ_g and τ_q at lower temperatures indicate the higher values of $\alpha_s(T)$ as compared to fixed, $\alpha_s = 0.3$, at those range of temperatures. However, at higher temperatures, the much lower values of $\alpha_s(T)$ ($\sim$0.18 at $T/T_c \gtrsim 5$), modulate the value of thermal relaxation times as compared to the fixed coupling. Clearly, the logarithmic term, containing α_s, playing the key role in determining the behavior of τ's while plotted as a function of temperature. Second, in order to visualize the EOS effects in the relaxation times, we introduced the quasiparticle distribution functions from Eq. (1) in the expressions of τ_g and τ_q along with effective couplings discussed in Sec. II. Both hard thermal loop (HTL) pQCD EOS for order $O(g^5)$ and $O(g^6 \ln(1/g) + \delta)$ (EOS1 and EOS2) and the 3-flavor lattice QCD EOS (LEOS) have been considered while implementing the quasiparticle properties in the QGP. Finally, We have observed that at higher temperatures, where the effective couplings ($\alpha_{\rm eff}$) using the HTL and lattice EOS becomes comparable to $\alpha_s(T)$, the respective plots of τ's almost merge with each other. However, since at $T/T_c \sim 8 - 10$, $\alpha_{\rm eff}$ becomes much smaller ($\sim$0.15), the α_s^2 term in the expression of τ's becomes somewhat predominant to keep the values of τ's a little above the running $\alpha_s(T)$ case. At lower temperatures, the values remain closer to fixed α_s case as the effective coupling becomes closer to 0.3. Therefore, it is crucial to mention that throughout the range of temperatures, the logarithmic term containing α_s in the denominator is playing a predominant role as well as the temperature behavior of the thermal relaxation times of quarks and gluons.

Before presenting the results of electrical conductivity using the thermal relaxation times including the leading log terms discussed so far, we present σ_{el} using the pQCD cross-section taken from Ref. [69]. The infrared singularity here regularized by the Debye mass m_D to obtain the cross section as $\frac{d\sigma}{dt} = \frac{d\sigma}{dq_\perp^2} \simeq \frac{\alpha_s^2}{(q_\perp^2 + m_D^2)^2}$, where $q_\perp$ is the transverse

component of momentum transfer which for small angle scattering $q_\perp^2 \approx -t$. In a number of recent works, this cross section has been used in order to determine the σ_{el} and other transport coefficients as well [26,27]. We see that the effect of coupling entering in the expression of differential scattering cross section as α_s^2 [the predominant logarithmic term $\ln(1/\alpha_s)$ is absent there]. Employing this cross section we have plotted σ_{el}/T as a function of T in Fig. 4 for a number of EOSs and compare them with some other estimations of electrical conductivity too. We observe that for ideal EOS and constant α_s, the ratio of electrical conductivity over temperature σ_{el}/T, is a constant over T. This is not unexpected as the there is no other temperature dependence due to the ideal EOS (the numerical value is close to ∼0.06 as indicated by the red dasher line). Implementing the running $\alpha_s(T)$ for ideal EOS, we observe that the larger values of α_s at lower temperatures are decreasing σ_{el}/T. This is due to the α_s^2 term in the cross section, that is appearing in the denominator of the expression of the σ_{el}. At lower temperatures, the above mentioned trend agrees with the results of Boltzmann Approach for Multi-Parton Scattering [25] and Greco *et al.* [26]. However, the smaller values of $\alpha_s(T)$ at larger temperatures are making σ_{el}/T enhanced with respect to fixed α_s case. Next, we have implemented the effects of EOS in both the distribution functions and in couplings while determining σ_{el}. At lower temperatures since $\alpha_{\rm eff}$ is smaller than $\alpha_s(T)$, σ_{el}/T exhibits larger values demonstrating the equation of state effects on electrical conductivity. At larger temperatures we can see that these plots almost merges with the one using ideal EOS and running $\alpha_s(T)$, since in those ranges of temperatures $\alpha_{\rm eff}/\alpha_s$ approaches to unity. Up to $T/T_c \sim 2$ we plotted lattice results from Aarts *et al.* [19]. The quantitative estimations of σ_{el}/T with quasiparticle EOSs agrees with the order of magnitude of the lattice results.

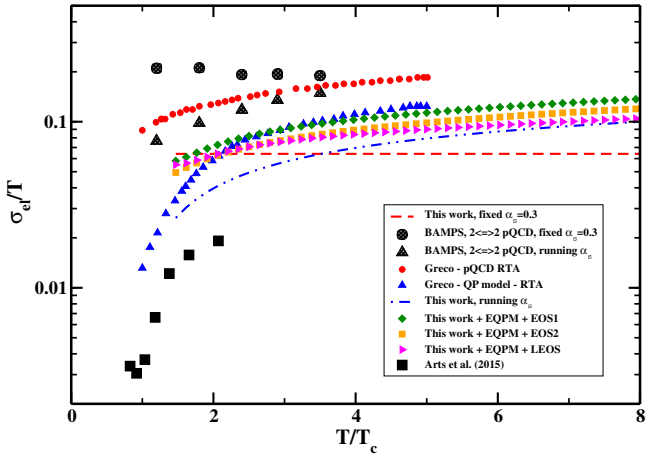

FIG. 4. The electrical conductivity scaled with temperature, σ_{el}/T for 3-flavor pQCD cross section as a function of T/T_c employing different EOSs.

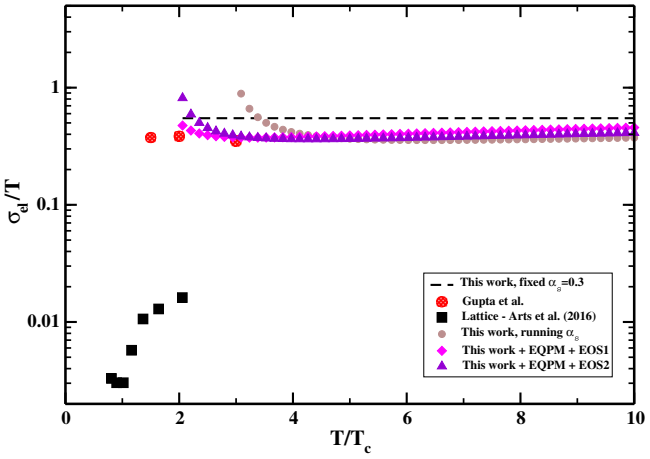

FIG. 5. The electrical conductivity scaled with temperature, σ_{el}/T for 2-flavor leading-log cross section as a function of T/T_c employing different EOSs.

Next, we present the results of electrical conductivity using the thermal relaxation times from Eqs. (21) and (22) including the leading log cross sections in Figs. 5 and 6. Due to the predominant contribution from the logarithmic term over coupling the magnitude of σ_{el}/T becomes quite larger than the pQCD case. In this case we have plotted σ_{el}/T both for 2- and 3-flavors individually for different EOSs and the 3-flavor case appears to be slightly greater since the quark charge q_Q^2 in Eq. (50) contains the fractional quark charge of strange quark also. The values of electrical conductivity with quasiparticle EOS and including $\alpha_{\rm eff}$ as the coupling show smaller values with respect to the one with ideal EOS and running $\alpha_s(T)$ at lower values of temperature due to the leading log effect. However at higher temperatures the two sets of curves merge with each other due to the fact that at large T, $\alpha_{\rm eff}$ approaches to running $\alpha_s(T)$. Although in this case at lower T/T_c the

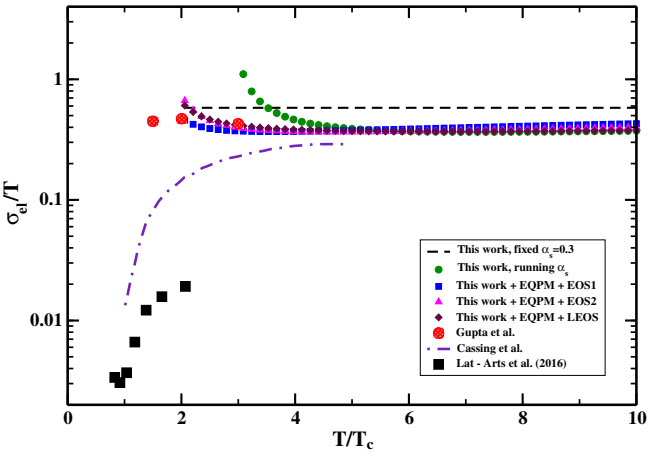

FIG. 6. The electrical conductivity scaled with temperature, σ_{el}/T for 3-flavor leading-log cross section as a function of T/T_c employing different EOSs.

lattice data from [19] quite underpredicts the results, the quenched lattice measurement of electrical conductivity from Gupta *et al.* [20] up to $T/T_c \sim 3$ remarkably agrees with the current estimation of σ_{el}. For 3-flavor case beyond $T/T_c \sim 3$, the estimations of σ_{el} is observed to match with the trend given in Cassing *et al.* [28] and agrees with their statement that above $T \sim 5T_c$ the dimensionless ratio σ_{el}/T becomes approximately constant (≈0.3). In all the above estimations of σ_{el} the electronic charges are explicitly multiplied using $\frac{e^2}{4\pi} = \frac{1}{137}$.

The diffusion coefficient D estimated from Eq. (55) multiplied with $2\pi T$, has been plotted for 2 and 3-flavor cases as a function of temperature in Figs. 7 and 8 respectively. In both the cases the values of diffusion coefficients have been compared with the lattice results provided by Aarts *et al.* [19]. Although in this case, the q_Q^2 term containing the flavor sum over fractional quark charges are absent, the flavor information is embedded in the thermal relaxation times in l_{11} term. Since for larger quark degeneracy, τ_q decreases, therefore, for 3-flavor case the values of D appear to be smaller than the 2-flavor case. Similar to the case of electrical conductivity, the leading log results for the diffusion coefficient turn out to be much higher due to the logarithmic term as compare to situation where only α_s^2 is present. The pQCD results are however closer to the lattice results. The quasiparticle model including the HTL and the lattice EOSs is observed to effect the values of D in a significant way. In the 3-flavor case, we also compare our results with the estimations of D using the holographic model from [31], which are in the range of temperature 0.2–0.4 GeV and agree well in the order of magnitude with our pQCD results. Finally, we have plotted the charge susceptibility as a function of temperature including ideal EOS and the EOSs described by EQPM in Fig. 9. In lower temperature region, ranging from 0.2–0.35 GeV, our results show good agreement with the lattice data from [21]. Different EOSs within

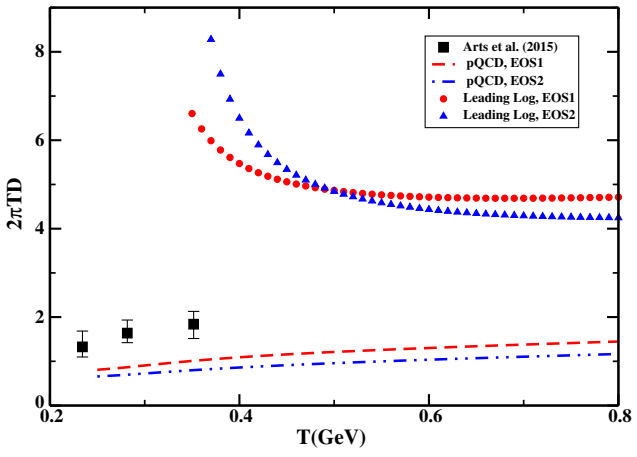

FIG. 7. Scaled charge diffusion coefficient, $2\pi DT$ for 2-flavor using pQCD and leading-log cross sections as a function of T employing various EOSs.

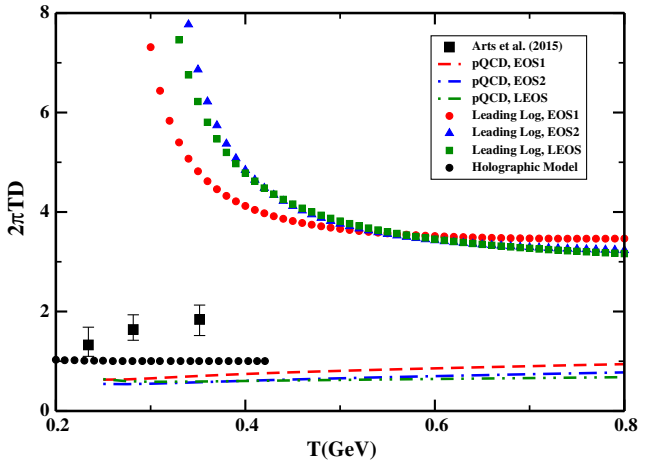

FIG. 8. Scaled diffusion coefficient, $2\pi DT$ for 3-flavor using pQCD and leading-log cross sections as a function of T employing various EOSs.

EQPM show discrete effects on χ. Interestingly, the ones with LEOS are closer to the lattice data the most. However, like any other quasiparticle model predictions, the EQPM predictions on the transport coefficients obtained here, show poor matching. This can perhaps be improved a bit while updating the temperature dependence of effective fugacities in our EQPM with more recent lattice results. Let us enlist the possible route causes of this discrepancy, specifically, in the context of our results on EM transport coefficients against the lattice results of Aarts *et al.* [19]. The first and foremost reason is the very philosophy to map hot QCD medium effects in terms of noninteracting/weakly interacting quasiparticle models for the temperatures closer to T_c where the interaction measure has a peak (although, at the level of fitting with the quasiparticle models and yields hot QCD thermodynamics, the matching the reasonably better, however, the very existence of the quasiparticle picture is in serious doubt). Another aspect is clearly the presence of the leading log term in the interaction cross section that follows from the infrared shielding discussed in Sec. II B. We have observed that this term is having the most significant contribution in controlling the temperature behavior of the relaxation times as well as transport parameters. The resulting enhancement of the temperature dependence of σ_{el} and D over the leading order pQCD results shown, is also responsible for the discrepancies of the current results with the lattice results provided by Aarts *et al.* [19].

There are more recent lattice data with the refined lattices both from HOT QCD collaboration [70] and Budapest-Marseille-Wuppertal Collaboration [71]. In fact, there are significant differences on the QCD trace anomaly near T_c between these two collaborations and also on T_c itself. Interpreting them in terms of EQPM and comparing the EM responses studied in this work and other transport coefficients of the QGP would be a matter of future investigations. Notably, at the level of EQPM, one requires to have lattice

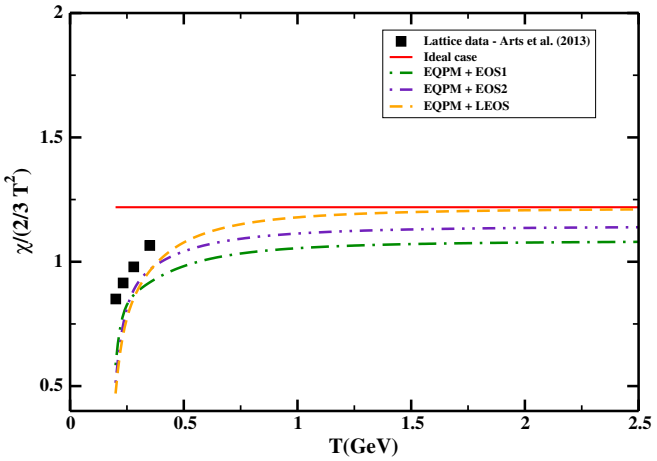

FIG. 9. Susceptibility, χ for 3-flavor using pQCD and leading-log cross sections as a function of T employing various EOSs.

results on trace anomaly for the pure glue sector (needed for defining z_g). Once the EQPM description is obtained for above mentioned lattice results, comparison with the predictions from direct lattice QCD method would prevail better understanding on the predictive power of the model.

IV. CONCLUSION AND OUTLOOK

The estimation of the transport coefficients that characterize the response of EM field to the electromagnetically charged QGP in the heavy-ion collisions, with realistic hot QCD/QGP equations of state (via their quasiparticle understanding), has led us to very interesting outcomes highlighting the impact of hot QCD medium effects. We have investigated the charge transport by determining the electrical conductivity of the QGP along with a related phenomenon of charge diffusion in the QGP medium by analyzing the charge diffusion coefficient.

The hot QCD medium effects have been included through the effective quasiparton distribution functions along with the effective coupling in QCD at high temperature. All the transport coefficients that have been investigated in this work, are influenced significantly in the presence of hot QCD medium effects coming from the various equations of state under consideration, as compared to the case of ideal equation of state for the QGP. The results obtained here are seen to be consistent with the outcomes of other approaches such as lattice QCD, dynamical quasiparticle models, holographic model based on AdS-CFT, transport theory and pQCD based studies discussed in the Introduction section.

The transport coefficients determined in this work and their temperature dependence could affect the quantitative estimates of the signals for the QGP from heavy ion collisions, particularly, where hydrodynamic simulations are involved. For example in Refs. [72–74], the soft photon emission rate is shown to be linearly dependent upon electrical conductivity. As a result the hydrodynamic description of the p_T spectra and elliptic flow of thermal photon and dileptons could be improved by including a realistic temperature dependence of the electrical conductivity. In that spirit relating the electrical conductivity and charge diffusion coefficients to the electromagnetic probes such as dilepton and photon production in relativistic heavy-ion collisions, and obtaining the spectra and collective flows would be a matter of immediate future investigations.

To achieve deeper understanding, the connections to the charge fluctuations and directed flow of charged hadrons in HIC would be another interesting aspect to explore in near future. In addition, extensions of the present analysis to estimate the other transport parameters such as shear and bulk viscosities, thermal conductivity along with generalizations in the case of anisotropic (momentum) hot QCD medium would be another direction where we shall intend to focus on.

ACKNOWLEDGMENTS

V. C. would like to acknowledge the funding from Department of Science and Technology, Government of India under Inspire Faculty Fellowship, IFA-13/PH-55. S. M. sincerely acknowledges IIT Gandhanhinagar, India for the Institute postdoctoral fellowship. People of India are sincerely acknowledged for their generous support for the research in basic sciences.

APPENDIX: CALCULATIONAL DETAILS OF CHAPMAN-ENSKOG METHOD

Starting from Eqs. (33) and utilizing the thermodynamic identities provided in Eq. (35), (36) and (37) and avoiding the terms containing velocity gradients that gives rise to viscous phenomena, we land in the following structure of transport equation,

$$\frac{1}{T}\Bigg[p_k^\nu \sum_{a=1}^{N'-1}(q_{ak}-x_a)\left\{(\nabla_\mu \mu_a)_{P,T}-\frac{h_a}{nh}\nabla_\mu P\right\} + p_k^\nu\{(p_k.u)-h_k\}\left\{\frac{\nabla_\mu T}{T}-\frac{\nabla_\mu P}{nh}\right\} + \left\{-(p_k\cdot u)(p_k\cdot E)\frac{\sum_{k=1}^N q_k n_k}{\sum_{k=1}^N h_k n_k}+q_k(p_k\cdot E)\right\}\Bigg] = -\frac{\omega_k}{\tau_k}\phi_k. \tag{A1}$$

The first two terms in the left-hand side of Eq. (A1) contribute to the diffusion driving force and thermal driving forces respectively for a system without the electric field effects. The third term purely arises from the effects of the electric field influencing the system. Now for generality it is desirable to express the electric filed driven terms in a manner, such that it resembles the thermal and diffusion driving terms. In this spirit we can decompose the third term in the following way,

$$\left\{-(p_k\cdot u)(p_k\cdot E)\frac{\sum_{k=1}^{N} q_k n_k}{\sum_{k=1}^{N} h_k n_k}+q_k(p_k\cdot E)\right\}$$
$$=p_k^{\nu}\{(p_k.u)-h_k\}X^E_{q\nu}+p_k^{\nu}\sum_{a=1}^{N'-1}(q_{ak}-x_a)X^E_{a\nu}. \quad \text{(A2)}$$

Here we have,

$$X^E_{q\mu}=-\frac{1}{h}\sum_{k=1}^{N}x_k q_k E_\mu, \quad \text{(A3)}$$

$$X^E_{k\mu}=\left[q_k-q_N-\frac{h_k-h_N}{h}\sum_{l=1}^{N}x_l q_l\right]E_\mu, \quad \text{(A4)}$$

as the thermal and diffusion driving forces only due to the influence of the electric field.

Applying the decomposition in Eq. (A1) we are finally able to get Eq. (38) with the complete expression of thermal and diffusion driving forces given in Eq. (39) and (40), respectively.

[1] J. Adams *et al.* (STAR Collaboration), Nucl. Phys. **A757**, 102 (2005); K. Adcox *et al.* (PHENIX Collaboration), Nucl. Phys. **A757**, 184 (2005); B. B. Back *et al.* (PHOBOS Collaboration), Nucl. Phys. **A757**, 28 (2005); I. Arsene *et al.* (BRAHMS Collaboration), Nucl. Phys. **A757**, 1 (2005).

[2] K. Aamodt *et al.* (The Alice Collaboration), Phys. Rev. Lett. **105**, 252302 (2010); Phys. Rev. Lett. **105**, 252301 (2010); Phys. Rev. Lett. **106**, 032301 (2011).

[3] P. Kovtun, D. T. Son, and A. O. Starinets, Phys. Rev. Lett. **94**, 111601 (2005).

[4] L. P. Csernai, J. I. Kapusta, and L. D. McLerran, Phys. Rev. Lett. **97**, 152303 (2006).

[5] R. A. Lacey, N. N. Ajitanand, J. M. Alexander, P. Chung, W. G. Holzmann, M. Issah, A. Taranenko, P. Danielewicz, and H. Stöcker, Phys. Rev. Lett. **98**, 092301 (2007).

[6] D. Kharzeev and K. Tuchin, J. High Energy Phys. 09 (2008) 093; F. Karsch, D. Kharzeev, and K. Tuchin, Phys. Lett. B **663**, 217 (2008); P. Romatschke and D. T. Son, Phys. Rev. D **80**, 065021 (2009); G. D. Moore and O. Saremi, J. High Energy Phys. 09 (2008) 015; C. Sasaki and K. Redlich, Phys. Rev. C **79**, 055207 (2009); Nucl. Phys. **A832**, 62 (2010).

[7] B. G. Zakharov, Phys. Lett. B **737**, 262 (2014); K. Tuchin, Phys. Rev. C **91**, 064902 (2015).

[8] K. Tuchin, Adv. High Energy Phys. **2013**, 490495 (2013).

[9] L. McLerran and V. Skokov, Nucl. Phys. **A929**, 184 (2014).

[10] U. Gürsoy, D. Kharzeev, and K. Rajagopal, Phys. Rev. C **89**, 054905 (2014).

[11] D. Satow, Phys. Rev. D **90**, 034018 (2014).

[12] B. Ling, T. Springer, and M. Stephanov, Phys. Rev. C **89**, 064901 (2014).

[13] Y. Hirono, M. Hongo, and T. Hirano, Phys. Rev. C **90**, 021903 (2014).

[14] M. Greif, F. Reining, I. Bouras, G. S. Denicol, Z. Xu, and C. Greiner, Phys. Rev. E **87**, 033019 (2013).

[15] A. Dobado, F. J. Llanes-Estrada, and J. M. Torres Rincon, arXiv:hep-ph/0702130.

[16] M. S. Green, J. Chem. Phys. **22**, 398 (1954); R. Kubo, J. Phys. Soc. Jpn. **12**, 570 (1957).

[17] G. Aarts, C. Allton, J. Foley, S. Hands, and S. Kim, Phys. Rev. Lett. **99**, 022002 (2007).

[18] A. Amato, G. Aarts, C. Allton, P. Giudice, S. Hands, and J. I. Skullerud, Phys. Rev. Lett. **111**, 172001 (2013).

[19] G. Aarts, C. Allton, A. Amato, P. Giudice, S. Hands, and J. I. Skullerud, J. High Energy Phys. 02 (2015) 186.

[20] S. Gupta, Phys. Lett. B **597**, 57 (2004).

[21] P. Giudice, G. Aarts, C. Allton, A. Amato, S. Hands, and J. I. Skullerud, *Proc. Sci.*, LATTICE (2014) 492 [arXiv:1309.6253].

[22] B. B. Brandt, A. Francis, H. B. Meyer, and H. Wittig, *Proc. Sci.*, ConfinementX (2012) 186 [arXiv:1302.0675].

[23] A. Francis and O. Kaczmarek, Prog. Part. Nucl. Phys. **67**, 212 (2012).

[24] P. V. Buividovich, M. N. Chernodub, D. E. Kharzeev, T. Kalaydzhyan, E. V. Luschevskaya, and M. I. Polikarpov, Phys. Rev. Lett. **105**, 132001 (2010).

[25] M. Greif, I. Bouras, and C. Greiner, Phys. Rev. D **90**, 094014 (2014).

[26] A. Puglisi, S. Plumari, and V. Greco, Phys. Lett. B **751**, 326 (2015).

[27] A. Puglisi, S. Plumari, and V. Greco, J. Phys. Conf. Ser. **612**, 012057 (2015).

[28] W. Cassing, O. Linnyk, T. Steinert, and V. Ozvenchuk, Phys. Rev. Lett. **110**, 182301 (2013).

[29] T. Steinert and W. Cassing, Phys. Rev. C **89**, 035203 (2014).

[30] S. X. Qin, Phys. Lett. B **742**, 358 (2015).

[31] S. I. Finazzo and R. Rougemont, Phys. Rev. D **93**, 034017 (2016).

[32] P. K. Srivastava, L. Thakur, and B. K. Patra, Phys. Rev. C **91**, 044903 (2015).

[33] D. Fernandez-Fraile and A. Gomez Nicola, Phys. Rev. D **73**, 045025 (2006).

[34] M. Greif, C. Greiner, and G. S. Denicol, Phys. Rev. D **93**, 096012 (2016).

[35] Vinod Chandra, R. Kumar, and V. Ravishankar, Phys. Rev. C **76**, 054909 (2007); **76**, 069904(E) (2007); Vinod Chandra, A. Ranjan, and V. Ravishankar, Eur. Phys. J. A **40**, 109 (2009).

[36] Vinod Chandra and V. Ravishankar, Phys. Rev. D **84**, 074013 (2011).

[37] A. Peshier, B. Kämpfer, O. P. Pavlenko, and G. Soff, Phys. Lett. B **337**, 235 (1994); Phys. Rev. D **54**, 2399 (1996).
[38] A. Peshier, B. Kämpfer, and G. Soff, Phys. Rev. C **61**, 045203 (2000); Phys. Rev. D **66**, 094003 (2002); V. M. Bannur, Phys. Rev. C **75**, 044905 (2007); **78**, 045206 (2008); J. High Energy Phys. 09 (2007) 046; A. Rebhan and P. Romatschke, Phys. Rev. D **68**, 025022 (2003); M. A. Thaler, R. A. Scheider, and W. Weise, Phys. Rev. C **69**, 035210 (2004); K. K. Szabo and A. I. Toth, J. High Energy Phys. 06 (2003) 008.
[39] M. DÉlia, A. Di Giacomo, and E. Meggiolaro, Phys. Lett. B **408**, 315 (1997); Phys. Rev. D **67**, 114504 (2003); P. Castorina and M. Mannarelli, Phys. Rev. C **75**, 054901 (2007); Phys. Lett. B **644**, 336 (2007); Paolo Alba *et al.*, Nucl. Phys. **A934**, 41 (2014).
[40] A. Dumitru and R. D. Pisarski, Phys. Lett. B **525**, 95 (2002); K. Fukushima, Phys. Lett. B **591**, 277 (2004); S. K. Ghosh, T. K. Mukherjee, M. G. Mustafa, and R. Ray, Phys. Rev. D **73**, 114007 (2006); H. Abuki and K. Fukushima, Phys. Lett. B **676**, 57 (2009); H. M. Tsai and B. Müller, J. Phys. G **36**, 075101 (2009).
[41] M. Bluhm, B. Kampfer, and K. Redlich, Phys. Rev. C **84**, 025201 (2011).
[42] Vinod Chandra and V. Ravishankar, Eur. Phys. J. C **64**, 63 (2009); **59**, 705 (2009).
[43] Vinod Chandra, Phys. Rev. D **86**, 114008 (2012); **84**, 094025 (2011).
[44] P. Chakraborty and J. I. Kapusta, Phys. Rev. C **83**, 014906 (2011).
[45] Albright and J. I. Kapusta, Phys. Rev. C **93**, 014903 (2016).
[46] A. Puglisi, S. Plumari, and V. Greco, Phys. Lett. B **751**, 326 (2015).
[47] S. Ryu, J.-F. Paquet, C. Shen, G. S. Denicol, B. Schenke, S. Jeon, and C. Gale, Phys. Rev. Lett. **115**, 132301 (2015).
[48] G. Denicol, A. Monnai, and B. Schenke, Phys. Rev. Lett. **116**, 212301 (2016).
[49] M. Cheng *et al.*, Phys. Rev. D **77**, 014511 (2008).
[50] M. Cheng *et al.*, Phys. Rev. D **77**, 014511 (2008); A. Bazavov *et al.*, Phys. Rev. D **80**, 014504 (2009); M. Cheng *et al.*, Phys. Rev. D **81**, 054504 (2010); S. Borsányi, G. Endrődi, Z. Fodor, A. Jakovác, S. D. Katz, S. Krieg, C. Ratti, and K. K. Szabó, J. High Energy Phys. 11 (2010) 077; Y. Aoki, Z. Fodor, S. D. Katz, and K. K. Szabó, J. High Energy Phys. 01 (2006) 089; J. High Energy Phys. 06 (2009) 088; S. Borsányi, Z. Fodor, C. Hoelbling, S. D. Katz, S. Krieg, C. Ratti, and K. K. Szabó, J. High Energy Phys. 09 (2010) 073.
[51] P. Arnold and C. Zhai, Phys. Rev. D **50**, 7603 (1994); **51**, 1906 (1995).
[52] C. Zhai and B. Kastening, Phys. Rev. D **52**, 7232 (1995).
[53] K. Kajantie, M. Laine, K. Rummukainen, and Y. Schroder, Phys. Rev. D **67**, 105008 (2003).
[54] P. F. Kelly, Q. Liu, C. Lucchesi, and C. Manuel, Phys. Rev. Lett. **72**, 3461 (1994); Phys. Rev. D **50**, 4209 (1994).
[55] D. F. Litim and C. Manual, Phys. Rep. **364**, 451 (2002).
[56] J. P. Blaizot and E. Iancu, Phys. Rep. **359**, 355 (2002).
[57] M. Laine and Y. Schöder, J. High Energy Phys. 03 (2005) 067.
[58] V. Chandra and V. Sreekanth, Phys. Rev. D **92**, 094027 (2015); arXiv:1602.07142.
[59] V. Chandra and V. Ravishankar, Nucl. Phys. **A848**, 330 (2010).
[60] V. Chandra and S. K. Das, Phys. Rev. D **93**, 094036 (2016); S. K. Das, V. Chandra, and Jan-e-Alam, J. Phys. G **41**, 015102 (2013).
[61] P. B. Arnold, G. D. Moore, and L. G. Yaffe, J. High Energy Phys. 11 (2000) 001.
[62] X. F. Zhang and W. Q. Chao, Nucl. Phys. **A628**, 161 (1998).
[63] B. L. Combridge, J. Kripfganz, and J. Ranft, Phys. Lett. **70B**, 234 (1977).
[64] M. H. Thoma, Phys. Rev. D **49**, 451 (1994).
[65] A. Hosoya and K. Kajantie, Nucl. Phys. **B250**, 666 (1985).
[66] S. R. De Groot, W. A. Van Leeuwen, and C. G. Van Weert, *Relativistic Kinetic Theory, Principles And Applications* (North-Holland, Amsterdam, Netherlands, 1980).
[67] M. Greif, Master Thesis, Goethe Universität, 2014.
[68] G. Baym, H. Monien, C. J. Pethick, and D. G. Ravenhall, Nucl. Phys. **A525**, 415C (1991).
[69] Z. Xu and C. Greiner, Phys. Rev. C **71**, 064901 (2005).
[70] A. Bazavov *et al.*, Phys. Rev. D **90**, 094503 (2014).
[71] S. Borsanyi, Z. Fodor, C. Hoelbling, S. D. Katz, S. Krieg, and K. K. Szabo, Phys. Lett. B **370**, 99 (2014).
[72] Y. Yin, Phys. Rev. C **90**, 044903 (2014).
[73] S. Caron-Huot, P. Kovtun, G. D. Moore, A. Starinets, and L. G. Yaffe, J. High Energy Phys. 12 (2006) 015.
[74] H.-T. Ding, A. Francis, O. Kaczmarek, F. Karsch, E. Laermann, and W. Soeldner, Phys. Rev. D **83**, 034504 (2011).